Static three-quark SU(3) and four-quark SU(4) potentials

C. Alexandrou
Department of Physics, University of Cyprus, CY-1678 Nicosia, Cyprus

Ph. de Forcrand
Inst. für Theoretische Physik, ETH Hönggerberg, CH-8093 Zürich, Switzerland
and CERN, Theory Division, CH-1211 Geneva 23, Switzerland

A. Tsapalis
Department of Physics, University of Athens, Athens, Greece

(Received 9 July 2001; published 31 January 2002)

We present results on the static three- and four-quark potentials in SU(3) and SU(4), respectively, within quenched lattice QCD. We use an analytic multihit procedure for the time links and a variational approach to determine the ground state. The three- and four-quark potentials extracted are consistent with a sum of two-body potentials, possibly with a weak many-body component at larger distances. For quark separations up to ~ 1.2 fm where the results are most accurate, we find support for the Δ *Ansatz* for the baryonic area law.

DOI: 10.1103/PhysRevD.65.054503 PACS number(s): 12.38.Gc

I. INTRODUCTION

The nature of the three-quark potential is of prime importance in the understanding of baryon structure. However up to now it has received little attention in lattice QCD studies. This is to be contrasted with the quark-antiquark potential relevant for meson structure for which many lattice results exist [1].

The aim of the present work is to study the nature of the three-quark potential within lattice QCD. The fundamental question, which was raised more than twenty years ago, is whether the static three-quark potential can be approximated by a sum of three two-body potentials, known in the literature as the Δ *Ansatz*, or whether it is a genuine three-body potential. The latter is obtained in the strong-coupling approximation by minimization of the energy of the three-quark state. The resulting minimal length flux tube is a configuration where the flux tubes from each quark merge at a point. Due to its shape it is known as the *Y Ansatz*.

Recently two lattice studies of the three-quark potential have reached different conclusions: Preliminary results by Bali [1] at $\beta=6.0$ favor the Δ *Ansatz* whereas the analysis of lattice results at $\beta=5.7$ by Takahashi *et al.* [2] gives more support to the *Y Ansatz*. The difficulty to resolve the dominant area law for the baryonic potential is due to the fact that the maximal difference between the two *Ansätze* is a mere 15%.

In our study we make a number of technical improvements in order to try and distinguish the *Y* and Δ *Ansätze*. In addition to using the standard techniques of smearing and the multihit procedure for noise reduction, we employ a variational approach [4] to extract the ground and first excited state of the three quarks. Both the multihit procedure, which is done analytically, and the variational approach were not used in Ref. [2]. These are especially important for the larger Wilson loops where the confining part of the potential is the most dominant. Instead of the multihit procedure for the time links we have also tried the recently proposed hypercubic blocking [5]. We did not, however, find any improvement as compared to the multihit procedure.

In addition to the SU(3) gauge group we also present results for SU(4). Since the same issues regarding the area law dependence of the Wilson loop arise in any gauge group, a calculation in SU(4) can help decide the preferred area law. The difference between the two-body approximation and the many-body force is bigger for SU(4), reaching a maximum value of 20% for the lattice geometries that we looked at.

The SU(3) baryon Wilson loop is constructed by creating a gauge invariant three-quark state at time $t=0$ which is annihilated at a later time T:

$$W_{3q}=\frac{1}{3!}\epsilon^{abc}\epsilon^{a'b'c'}U(x,y,1)^{aa'}U(x,y,2)^{bb'}U(x,y,3)^{cc'} \tag{1.1}$$

for the three quark lines that are created at x and annihilated at y and

$$U(x,y,j)=P\exp\left[ig\int_{\Gamma(j)}dx^{\mu}A_{\mu}(x)\right], \tag{1.2}$$

where P is the path ordering and $\Gamma(j)$ denotes the path from x to y for quark line j as shown in Fig. 1.

The three-quark potential is then extracted in the standard way from the long-time behavior of the Wilson loop:

$$V_{3q}=-\lim_{T\to\infty}\frac{1}{T}\ln\langle W_{3q}\rangle. \tag{1.3}$$

In SU(4) the corresponding color singlet gauge invariant four-quark state is constructed in an analogous manner and the four-quark potential V_{4q} is similarly extracted. We will be using the term baryonic potential to denote the color singlet combination of N quarks despite the fact that in SU(4) the spin of the four-quark state is an integer.

 ©2002 The American Physical Society

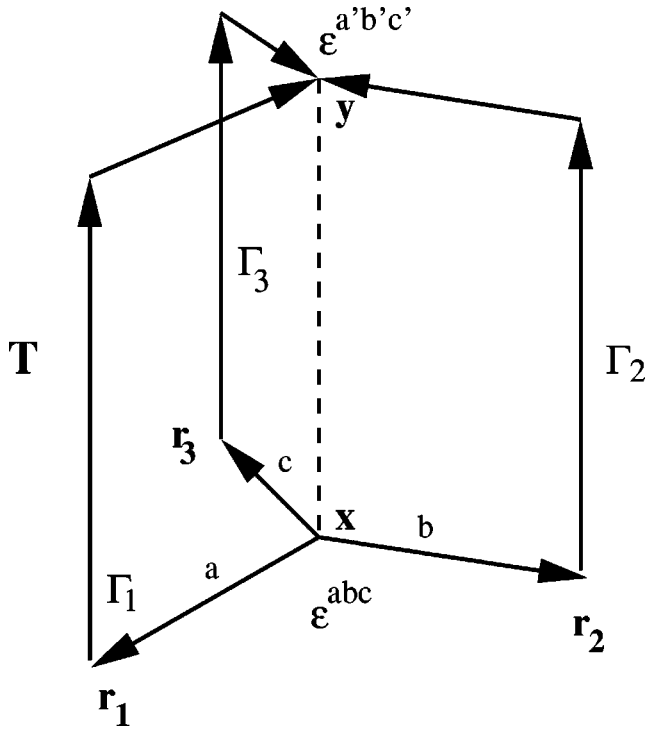

FIG. 1. The baryonic Wilson loop. The quarks are located at positions $\mathbf{r}_1$, $\mathbf{r}_2$, and $\mathbf{r}_3$.

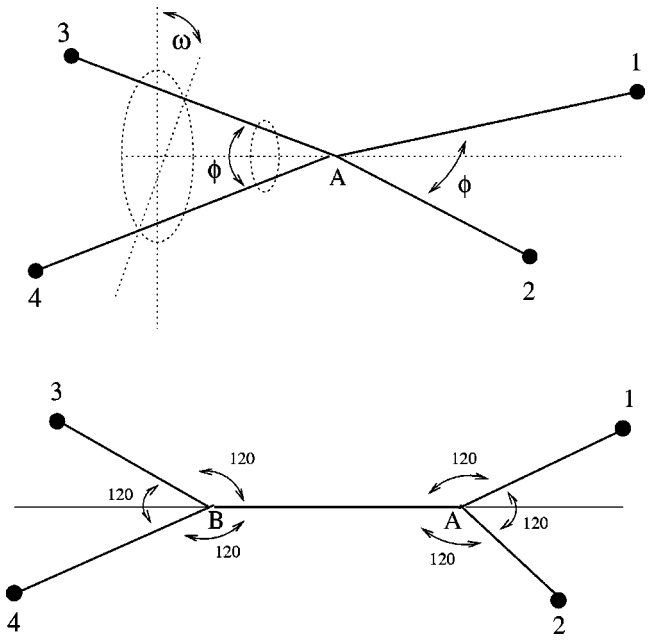

FIG. 2. The Wilson loop for four quarks. The quarks are located at positions $\mathbf{r}_1$, $\mathbf{r}_2$, $\mathbf{r}_3$, and $\mathbf{r}_4$. The upper graph shows the local minimum of the energy with one Steiner point *A*, and the lower is the minimum with two Steiner points *A* and *B*.

II. WILSON LOOP FOR THREE AND FOUR QUARKS

A. SU(3)

Here we describe in more detail the two possibilities put forward for the area law of the SU(3) baryon Wilson loop. In the strong-coupling limit in the presence of three heavy quarks the gauge invariant three-quark state with the least amount of flux will yield the lowest energy. If the three quarks are at positions $\mathbf{r_1}$, $\mathbf{r_2}$, and $\mathbf{r_3}$ and provided none of the interior angles of the triangle with vertices at the quark sites is greater than 120° then the flux tubes from the quarks will meet at an interior point $\mathbf{r}_4$ [6]. The position $\mathbf{r}_4$ is determined by minimizing the static energy with the result

$$\sum_{k=1}^{3} \frac{(\mathbf{r}_k - \mathbf{r}_4)}{|\mathbf{r}_k - \mathbf{r}_4|} = 0, \tag{2.1}$$

which is known as the Steiner point. The angles between the flux tubes are 120° independently of the vectors $\mathbf{r}_k$. If one of the interior angles of the triangle of the quarks is greater than 120° then the flux tube at that angle collapses to a point. Time evolution of this state produces a three-bladed area. This area law is the *Y Ansatz* mentioned in the Introduction. We denote the minimal length of the flux tube for this *Ansatz* L_Y and the corresponding area A_Y.

The second possibility [7] is that the relevant area dependence of the baryonic Wilson loop is given by the sum of the minimal areas A_{ij} spanning quark lines *i* and *j*. This is known as the Δ *Ansatz* with the corresponding length and area denoted by L_Δ and A_Δ, respectively.

The position of the Steiner point can be obtained analytically [6] in terms of the three-quark positions and the difference between the two laws as compared to the two-body *Ansatz*,

$$\left(\sum_j r_{j4} - \frac{1}{2} \sum_{j<k} r_{jk} \right) \Big/ \frac{1}{2} \sum_{j<k} r_{jk}, \tag{2.2}$$

attains [6] the maximum value of $(L_Y - L_\Delta/2)/(L_\Delta/2) = 2/\sqrt{3} - 1 = 0.15$ when the quarks form an equilateral triangle. The factor of 1/2 is due to the non-Abelian nature of the gauge couplings giving half as much attraction for a qq in an antisymmetric color state as a $q\bar{q}$ in a color singlet. In general the attraction for $(N-1)$ quarks in an N quark antisymmetric color state is a factor $1/(N-1)$ less than the attraction for a $q\bar{q}$ in a color singlet. Because of this factor $L_\Delta/(N-1) \leqslant L_Y$.

B. SU(4)

In SU(4) the ground state of the system in strong coupling corresponds to the configuration with minimal length for the flux tubes which join the quarks. Minimization of the static energy results in the introduction of two Steiner points, *A* and *B*, somewhere in space, with the flux tubes from two quarks joining at *A*, while the flux tubes from the other two quarks meet at *B*. This configuration is visualized in Fig. 2. Since $4 \times 4 = 6 \oplus 10$ the two lines emanating from the two Steiner points join to form a color singlet. In analogy to SU(3) we will call this area law the *Y Ansatz*, with a corresponding flux tube length L_Y.

In addition to the configuration with two Steiner points there is another possible configuration with a single Steiner point defined by the following equation:

$$\sum_{k=1}^{4} \frac{(\mathbf{r}_k - \mathbf{r}_A)}{|\mathbf{r}_k - \mathbf{r}_A|} = 0, \tag{2.3}$$

where all four quark lines meet. The area law for the baryonic Wilson loop now takes the shape of a long four-bladed surface with the blades meeting at A as shown in Fig. 2. Due to this shape, we refer to this configuration as the X law and denote the corresponding flux tube length as L_X.

In contrast to SU(3) where for any given location of the three quarks, the Steiner point and therefore the energy can be computed analytically, in SU(4), the two Steiner points in the *Y Ansatz* can be obtained by an iterative numerical procedure. To keep this procedure simple, we assume that the double string between the two Steiner points has the same tension as the other four, single strings. In fact, the tension of the double string is 1.357(29) times greater [8]. Thus, we introduce a small, but systematic error. Since its effect is to reduce the potential of the *Y Ansatz*, it has no bearing on our conclusions. The two Steiner points then have vectors that each meet at 120° and one Steiner point can be obtained in terms of the other. Starting from an initial guess for the position of one of the Steiner points, $\mathbf{r}_A$, we can compute $\mathbf{r}_B$ as the Steiner point of $\mathbf{r}_3$, $\mathbf{r}_4$, and $\mathbf{r}_A$. The $\mathbf{r}_1$, $\mathbf{r}_2$, and $\mathbf{r}_B$ vectors lead now to a new estimate for a Steiner point $\mathbf{r}_A$ which in turn is used to compute a new $\mathbf{r}_B$, etc. (The procedure converges after 30–40 iterations to the minimum.) The location of the single Steiner point is easily computed by a numerical solution to Eq. (2.3).

It has been argued in [7] that the two-body force is the relevant interaction for any SU(N) gauge theory. It is proven in [7] that $L_Y \geqslant L_\Delta/(N-1)$ holds for any location of the four quarks. From the numerical investigation, it turns out that the relative difference between the Y energy and the two-body law is maximal for the configuration of maximal symmetry for the four quarks. This amounts to putting the quarks on the vertices of the regular tetrahedron and gives a relative difference of 21.96% with respect to the two-body term. This difference decreases as the configuration becomes more asymmetric in space and can decrease down to 5–6% for the most asymmetric locations of the quarks on a 16^3 lattice. Therefore, in order to obtain a clear signal on which law is preferred by the SU(4) quarks, we studied geometries with maximal symmetry.

As far as the four-bladed surface area law is concerned, we observed that L_X always exceeds L_Y by at most 3.5%. In fact, the ratio, $(L_X - L_Y)/L_Y$, becomes minimal for the most symmetric configuration of the tetrahedron, obtaining a value of just 0.43%. Here the ratio in fact increases as one increases the asymmetry of the four-quark locations, becoming maximal if all four quarks are located on a plane. In particular, if the quarks are located at the vertices of a square, $(L_X - L_Y)/L_Y$ takes its maximal value of 3.5%. With the current data, discriminating an effect of $\mathcal{O}(3)$% between the *Y Ansatz* and the *X Ansatz* is not possible. This remains true even if we take the larger value for σ for the double string in the two Steiner configuration. Therefore, we will pick geometries that maximize the difference between the Y and Δ *Ansätze*. Since for these geometries the difference between the Y and *X Ansätze* is of the order of 2% one has to keep in mind that when we refer to the *Y Ansatz* we will in fact mean the area law with one or two Steiner points.

The factor of $1/(N-1)$ which relates the long-range part of the two-body $q\bar{q}$ and qq potentials also occurs in lowest order gluon exchange so that the two-body short-range potential is given by [7]

$$\frac{1}{(N-1)} \sum_{j<k} V_{jk}, \tag{2.4}$$

where V_{jk} is the $q\bar{q}$ one-gluon potential

$$V_{jk} = -\frac{g^2 C_F}{4\pi r_{jk}} \tag{2.5}$$

with $C_F = (N^2-1)/2N$ the quark Casimir of $O(N)$.

Thus the expected forms of the ''baryonic'' potential in SU(N) that we will be applying to SU(3) and SU(4) are

$$V_{Nq}(\mathbf{r}_1, \ldots, \mathbf{r}_N) = \frac{N}{2} V_0 - \frac{1}{N-1} \sum_{j<k} \frac{g^2 C_F}{4\pi r_{jk}} + \frac{1}{N-1} \sigma L_\Delta \tag{2.6}$$

or

$$V_{Nq}(\mathbf{r}_1, \ldots, \mathbf{r}_N) = \frac{N}{2} V_0 - \frac{1}{N-1} \sum_{j<k} \frac{g^2 C_F}{4\pi r_{jk}} + \sigma L_Y \tag{2.7}$$

with σ the string tension of the $q\bar{q}$ potential.

III. LATTICE TECHNIQUES

As we mentioned in the Introduction, the two recent lattice studies of the baryonic potential [2,1] have yielded different conclusions, the first supporting the *Y Ansatz* and the second the Δ *Ansatz*. Since the difference between the two *Ansätze* is $\sim$15% for SU(3), obtaining conclusive results requires making a large effort to reduce the statistical noise, especially for the large loops where the absolute difference between the two *Ansätze* becomes more visible. In this work, we used a number of improvements as compared to previous studies in SU(3). To our knowledge, this is the first measurement of the 4-quark potential in SU(4). We describe briefly the techniques that we use in order to reduce noise and extract more reliably the ground state.

We use the multihit procedure [9] for the time links. For SU(3) the temporal links are integrated out analytically [3] and substituted by their average value

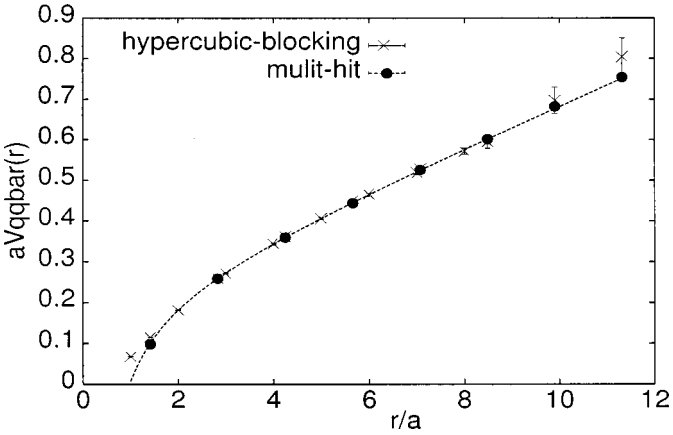

FIG. 3. The $q\bar{q}$ potential for SU(3) at $\beta=6.0$ on a $16^3\times 32$ lattice using the multihit procedure (filled circles) symbol and hypercubic blocking (crosses).

$$U_4(x)\to\overline{U}_4(x)=\frac{\int dU\, U_4(n)e^{\beta S_4(U)}}{\int dU\, e^{\beta S_4(U)}} \tag{3.1}$$

with $S_4(U)=(1/N)\mathrm{Tr}[U_4(n)F^\dagger(n)]$ and $F(n)$ is the staple attached to the time link that is being integrated over. It has been shown in SU(2) [9] that replacing the time links by their average value in this fashion reduces the error on large Wilson loops of the order of tenfold. The factor found in Ref. [9] is $x^{2T}\sim 0.889^{2T}$, where T is the time extent of the Wilson loop. For the SU(3) baryon loop the reduction factor will be x^{3T} giving an even larger noise reduction for the large loops. Here we point out that the multihit procedure was not used in Ref. [2]. In SU(4) the integration over the temporal links was done numerically.

We compared the multihit procedure with the recently proposed hypercubic blocking [5] on the time links. Using the optimal parameters given in [5] at $\beta=6.0$, we compare in Fig. 3 the results on the same configurations, using the analytic multihit procedure and using hypercubic blocking. As can be seen, the multihit procedure gives smaller errors for large loops and therefore we adopt it in this work.

To maximize the overlap of the trial state with the three-quark ground state we use smearing of the spatial links [10]. We replace each spatial link by a fat link by acting on it with the smearing operator $\mathcal{S}$ defined by

$$\mathcal{S}U_j(x)=\mathcal{P}\left(U_j(x)+\alpha\sum_{k\neq j}[U_k(x)U_j(x+a\hat{k})U_k^\dagger(x+a\hat{j})]\right), \tag{3.2}$$

where $\mathcal{P}$ denotes the projection onto SU(3). This is iterated n times. We consider M different levels of smearing and construct an $M\times M$ correlation matrix of Wilson loops [11]. For the parameter α and the number of smearings, n_l, for each different smearing level l we take what is found to be optimal in [11], namely,

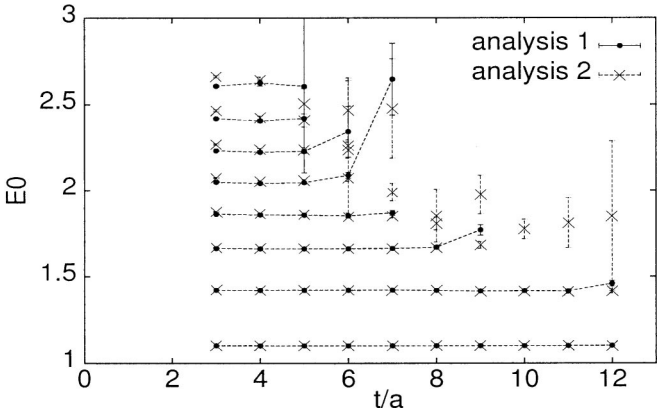

FIG. 4. Comparison of the plateaus obtained in SU(4) for $-\ln[\lambda_0(t+1)/\lambda_0(t)]$ solving the generalized eigenvalue equation at each time t (filled circles) and with the projected Wilson loop $-\ln[W_P(t+1)/W_P(t)]$ (crosses). The line is drawn to guide the eye.

$$\alpha=\frac{1}{2},\quad n_l\approx\frac{l}{2}\left(\frac{r_0}{a}\right)^2, \tag{3.3}$$

for smearing levels $l=0,\ldots,M-1$ and r_0 Sommer's reference scale [12]. In all our computations we used $M=4$. For SU(4) at $\beta=10.9$ we found that the parameters used for $\beta=5.8$ in SU(3) produce reasonable results.

The correlation matrices $C(t)$ for the mesonic and baryonic Wilson loops were analyzed using a variational method [4]. We use two different variants both yielding consistent results.

In both variants we solve the generalized eigenvalue problem [11]

$$C(t)v_k(t)=\lambda_k(t)C(t_0)v_k(t) \tag{3.4}$$

taking $t_0/a=1$. In the first variant, the potential levels are extracted via

$$aV_k=\lim_{t\to\infty}-\ln\left(\frac{\lambda_k(t+1)}{\lambda_k(t)}\right) \tag{3.5}$$

by fitting to the plateau. In the second variant we consider the projected Wilson loops

$$W_P(t)=v_0^T(t_0)C(t)v_0(t_0) \tag{3.6}$$

and fit to the plateau value of $-\ln[W_P(t+1)/W_P(t)]$. In Fig. 4 we show the results of these two variants for SU(4) for the four-quark static potential.

The projected correlation has a larger contamination of excited states for time slice $t/a=3$ but by the next time slice the two procedures yield the same results. We have found that for SU(3), where the n_l for the lth smearing level are larger for the corresponding β values than the number of smearings used in SU(4), the projected method yields smaller errors. In all cases we have checked that the values we extract for the ground state within these two procedures are consistent with each other. From Eq. (3.5) we also obtain the energy for the first-excited state. Although the data are rather noisy, we can obtain an estimate, which we use to fix

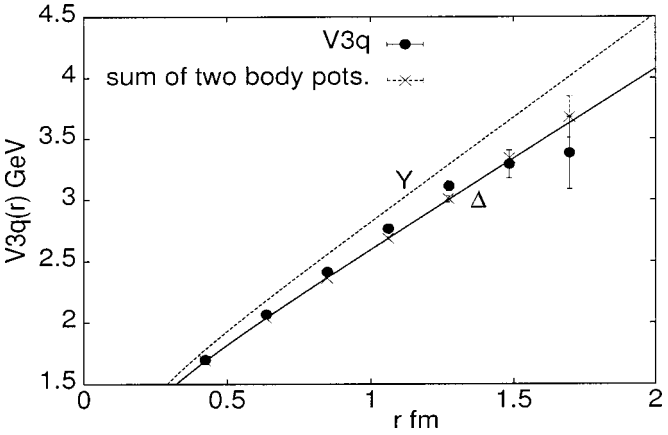

FIG. 5. The static baryonic potential at $\beta=5.8$ (filled circles) in physical units. The crosses are the sum of the static $q\bar{q}$ potential. The curves for the Δ and *Y Ansätze* are also displayed. The quarks are located at $(l,0,0)$, $(0,l,0)$, $(0,0,l)$, and $r=r_{12}=r_{13}=r_{23}=\sqrt{2}l$.

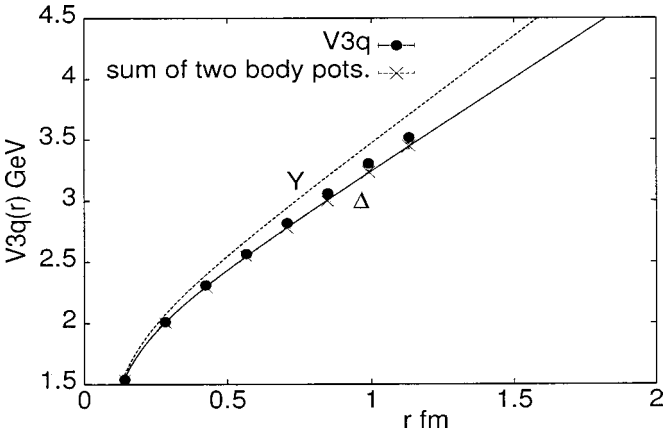

FIG. 6. The same as Fig. 5 but for $\beta=6.0$.

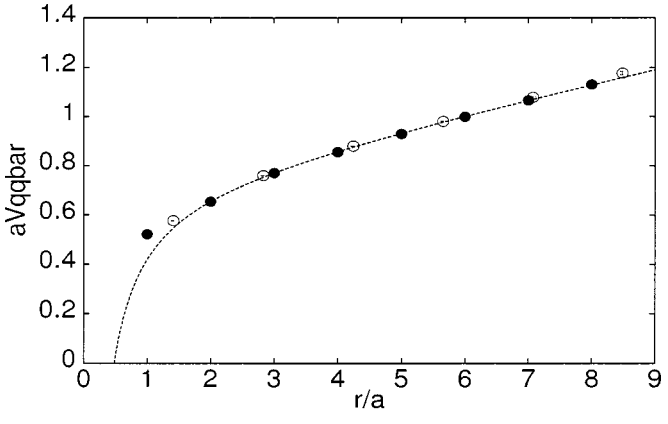

FIG. 7. The $q\bar{q}$ potential for SU(4) at $\beta=10.9$ fitted to the form $V_0-b/r+\sigma r$. The jackknife errors are comparable to the size of the symbols. The filled circles are data for the on-axis $q\bar{q}$ potential whereas the open circles give the potential when the q and $\bar{q}$ are on different axes equidistant from the origin.

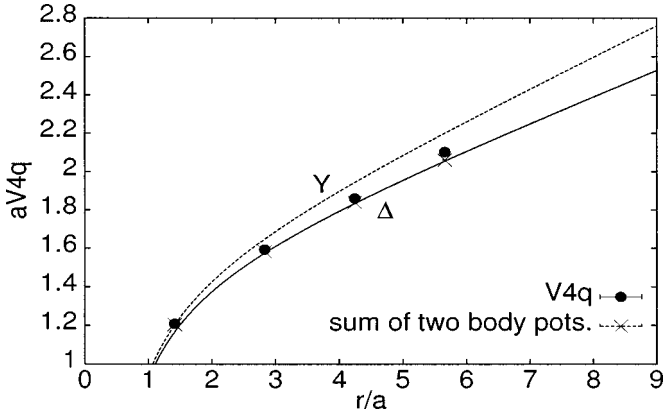

FIG. 8. The static baryon potential for SU(4) geometry 1 in lattice units. The notation is the same as that of Fig. 5. The quarks are located at $(l,0,0)$, $(0,l,0)$, $(-l,0,0)$, $(0,-l,0)$, and $r=r_{12}=r_{23}=r_{34}=r_{14}=\sqrt{2}l$.

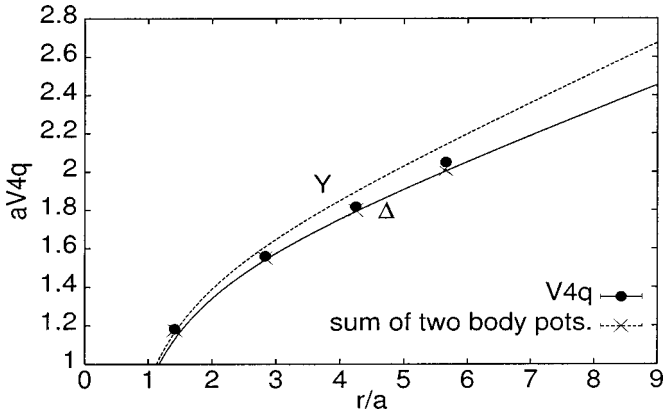

FIG. 9. As Fig. 8 but for geometry 2. Here the quarks are located at $(l,0,0)$, $(0,l,0)$, $(-l,0,0)$, $(0,0,l)$, and $r=r_{12}=r_{23}=r_{34}=r_{14}=\sqrt{2}l$.

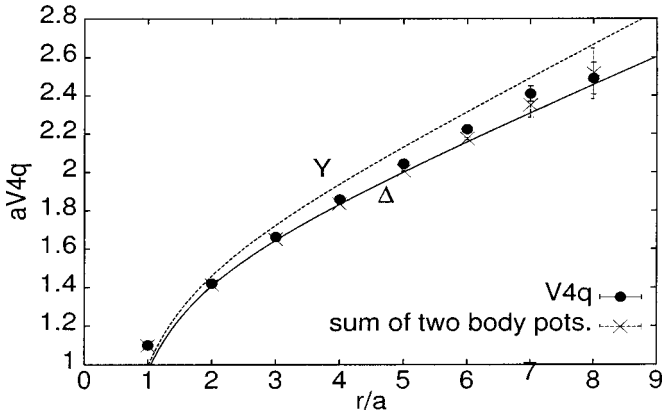

FIG. 10. As Fig. 8 but for geometry 3. The quarks are located at $(r,0,0)$, $(0,r,0)$, $(0,0,r)$, and $(0,0,0)$.

the minimum value for the time interval used in the extraction of the ground state, such that the excited state contamination is less than e^{-2}.

IV. RESULTS

All the computations were carried out on lattices of size $16^3 \times 32$ at β values 5.8 and 6.0 for SU(3) and 10.9 for SU(4). The β value for SU(4) was chosen so that the lattice spacing is close to the value for SU(3) at $\beta = 6.0$, assuming the same physical string tension. In the case of SU(3) we used 200 configurations at $\beta = 5.8$ and 220 at $\beta = 6.0$ available at the NERSC archive [13] and for SU(4) we generated 100 quenched configurations.

We consider geometries on the lattice which produce the biggest difference between the Δ and *Y Ansätze*. For SU(3) each quark is placed on a different spatial axis equidistant from the origin. The results are shown in Figs. 5 and 6 for $\beta = 5.8$ and 6.0, respectively. To reduce systematic errors when comparing with the $q\bar{q}$ potential, we also compute, on the same configurations, the static $q\bar{q}$ potential with the quark and the antiquark at the same locations as the three quarks of the qqq potential. The errors shown on these figures are the jackknife errors. The string tension in lattice units extracted from fitting the $q\bar{q}$ potentials is $a\sqrt{\sigma} = 0.329(3)$ at $\beta = 5.8$ and $0.224(3)$ at $\beta = 6.0$ consistent with the value of Ref. [14]. At short distances the baryonic potential, V_{3q}, is approximately equal to the sum of the corresponding two-body potentials, i.e., we find agreement with the tree level result that $V_{3q} \approx 3/2 V_{q\bar{q}}$. At larger distances, V_{3q} is enhanced compared to the tree level result. On the same figures we also show the curves corresponding to the Δ and *Y Ansätze*. The lattice data lie closer to the curve given by the Δ area law. However, at distances larger than about 0.7 fm, the three-quark potential appears enhanced as compared to the sum of the two-body potentials. This enhancement can be explained by a small admixture of a three-body force, although it is so small that it might also reflect imperfections in our variational search for the ground state.

In SU(4) we studied three different geometries chosen so that the difference between the Δ and analog of the *Y* law is maximal. In what we call geometry 1 the quarks are placed symmetrically on a plane distance l from the origin. The energy difference between the two *Ansätze* is 20.0%. In geometries 2 and 3, three quarks have coordinates $(l,0,0)$, $(0,l,0)$, and $(0,0,l)$ whereas the fourth is at $(0,0,-l)$ for geometry 2 and at the origin for geometry 3. The energy differences between the Δ and *Y* laws are 20.1% for geometry 2 and 19.1% for geometry 3. The string tension is obtained by fitting the on-axis $q\bar{q}$ potential excluding the first point. We find $a\sqrt{\sigma} = 0.238(4)$ in agreement with the value of 0.2429(14) of Ref. [15]. The quality of the fit is shown in Fig. 7 with χ^2/degree of freedom $= 1.0$, where we also included the results when the quark and the antiquark are on different axes.

The corresponding results for the four-quark static potential are shown in Figs. 8, 9, and 10 for geometries 1, 2, and 3, respectively. Again we find that the four-quark potential is approximated by the sum of $q\bar{q}$ potentials with a small enhancement at larger distances. The results in all cases lie closer to the Δ *Ansatz*.

V. CONCLUSIONS

Our results for the static three- and four-quark potential in SU(3) and SU(4) are consistent with the sum of two-body potentials below a distance of about 0.8 fm, and inconsistent with the *Y Ansatz* defined with the string tension extracted from the $q\bar{q}$ potential.

For larger distances, where our statistical and systematic errors both become appreciable, there appears to be a small enhancement due to an admixture of a many-body component. Nevertheless, for the distances up to 1.2 fm that we were able to probe in this work, the Δ area law gives the closest description of our data.

We have made use of all the known techniques in order to reliably identify the plateaus in the Wilson loops and extract the ground-state potential. Nevertheless, for the larger loops the plateaus were hard to identify, resulting in large errors. This is a challenging numerical problem, and we cannot exclude the possibility that the small enhancement of the potential above the Δ area law which we observe is simply caused by a failure to filter out all excited states in our variational search for the ground state. Taking the results in both SU(3) and SU(4) at face value the conclusion that can be drawn is that the Δ area law provides the closest description to the baryonic potential up to distances of 1.2 fm. More refined techniques for noise reduction for the large loops will be needed in order to clarify whether a genuine many-body component is present at larger distances.

ACKNOWLEDGMENTS

We thank E. Follana and H. Panagopoulos for discussions. A.T. wishes to thank the University of Cyprus for extended hospitality and financial support during stages of this research.

[1] G. S. Bali, Phys. Rep. **343**, 1 (2001).
[2] T. T. Takahashi, H. Matsufuru, Y. Nemoto, and H. Suganuma, Phys. Rev. Lett. **86**, 18 (2001).
[3] Ph. de Forcrand and C. Roiesnel, Phys. Lett. **151B**, 77 (1985).
[4] N. A. Campbell, A. Huntley, and C. Michael, Nucl. Phys. **B306**, 51 (1988); M. Lüscher and U. Wolff, *ibid.* **B339**, 222 (1990).
[5] A. Hasenfratz and F. Knechtli, Phys. Rev. D **64**, 034504 (2001).
[6] J. Carlson, J. Kogut, and V. R. Pandharipande, Phys. Rev. D **27**, 233 (1983).
[7] J. M. Cornwall, Phys. Rev. D **54**, 6527 (1996).
[8] B. Lucini and M. Teper, Phys. Rev. D **64**, 105019 (2001).
[9] G. Parisi, R. Petronzio, and F. Rapuano, Phys. Lett. **128B**, 418

(1983); G. S. Bali, K. Schilling, and Ch. Schlichter, Phys. Rev. D **51**, 5165 (1995).
[10] APE Collaboration, M. Albanese *et al.*, Phys. Lett. B **192**, 163 (1987).
[11] M. Guagnelli, R. Sommer, and H. Wittig, Nucl. Phys. **B535**, 389 (1998).
[12] R. Sommer, Nucl. Phys. **B411**, 839 (1994).
[13] NERSC archive, G. Kilcup *et al.*, Nucl. Phys. B (Proc. Suppl.) **53**, 345 (1997).
[14] G. S. Bali and K. Schilling, Phys. Rev. D **46**, 2636 (1992).
[15] B. Lucini and M. Teper, J. High Energy Phys. **06**, 050 (2001).